J Mater Sci (2006) 41:7853–7861
DOI 10.1007/s10853-006-0422-z

Magnetically controlled microstructure evolution in non-ferromagnetic metals

D. A. Molodov · P. J. Konijnenberg · L. A. Barrales-Mora · V. Mohles

Received: 17 February 2006 / Accepted: 8 May 2006 / Published online: 24 October 2006

Abstract The microstructure evolution during grain growth in magnetically anisotropic materials can be affected by a magnetic field due to an additional driving force for grain boundary motion which arises from a difference in magnetic free energy density between differently oriented grains. Therefore each grain of a polycrystal, exposed to a magnetic field, is inclined to grow or to shrink by a magnetic force depending on the orientation of the respective grain and its surrounding neighbors with regard to the field direction. A theoretical analysis of the grain growth kinetics in the presence of an external magnetic field reveals that magnetically affected grain growth may result in an orientation distribution that favours grains with a lower magnetic free energy density. As it is experimentally demonstrated on polycrystalline zinc, titanium and zirconium, the crystallographic texture in magnetically anisotropic non-magnetic materials can be effectively changed and controlled by means of annealing in a magnetic field. EBSD-analysis revealed that the observed asymmetrical texture after magnetic annealing is due to a large extent to a significant difference in the number of grains that make up different texture components. The results of computer simulations of magnetically affected grain growth in 2-D polycrystals are in a good agreement with theoretical predictions and experimental findings.

D. A. Molodov (✉) · P. J. Konijnenberg · L. A. Barrales-Mora · V. Mohles
Institute of Physical Metallurgy and Metal Physics, RWTH Aachen University, Kopernikusstr. 14, 52056 Aachen, Germany
e-mail: molodov@imm.rwth-aachen.de

Introduction

Properties of polycrystalline solids, in particular mechanical ones, depend on the size and spatial orientation of the grains inside. Both size and orientation distribution of these grains are subjected to changes in the course of grain growth after the completion of primary recrystallization. Grain growth proceeds by the migration of grain boundaries. An understanding of the response of grain boundaries to exerted forces is the key for an effective control of grain growth in crystalline solids. Such an understanding is therefore the basic requirement for a control of microstructure and properties, indispensable for the design of advanced materials for various engineering applications.

The grain microstructure evolution can be influenced by the application of an external field [1–3]. In particular, grain boundary motion can be affected by a magnetic field, owing to a driving force that arises in the field due to a crystal magnetic anisotropy. In literature most experimental observations of magnetically induced changes in recrystallization and texture development relate to ferromagnetic materials [2]. However, magnetic field effects on microstructure evolution are not restricted to ferromagnetics only. As shown in the past by Mullins [4, 5] and confirmed in our more recent bicrystalline experiments [6–9], also grain boundaries in non-magnetic materials (i.e. paramagnetic and diamagnetic) can be forced to move by a magnetic driving force, induced by a crystallographic anisotropy in magnetic susceptibility. Since this magnetic force does not depend on boundary properties and can be determined accurately, measurements of magnetically driven grain boundary motion gain access to the absolute value of grain boundary mobility and its

dependence on the grain boundary character [6–9]. Observations of magnetically induced selective grain growth in locally deformed zinc single crystals provided unambiguous evidence that the microstructure development in magnetically anisotropic non-magnetic materials can be controlled by magnetic annealing [10, 11]. Further experiments on polycrystalline cold-rolled zinc [12], titanium [13, 14] and zirconium [15] revealed that magnetic annealing can cause significant changes in the crystallographic texture of these materials. A magnetic field can therefore be effectively utilized as an additional degree of control of texture development in crystalline non-magnetic solids. In the current paper the microstructure evolution is addressed in non-magnetic materials during grain growth in the presence of an external magnetic field.

Driving forces

The driving force p for grain boundary migration arises if the boundary displacement is accompanied by a decrease of the total free energy of the system G: $p = -\mathrm{d}G/\mathrm{d}V$, where V is the volume swept by the boundary during its displacement. The driving force has therefore the dimension of energy per unit volume which is equivalent to a force per unit area.

The driving force for boundary motion during grain growth usually stems from the free energy of the boundary itself. A curved boundary reduces its area and therefore its free energy as it moves towards its center of curvature. For a boundary of energy γ with radii of curvature in two perpendicular sections r_1 and r_2 the driving force can be expressed as

$$p_{\mathrm{c}} = \gamma\left(\frac{1}{r_1}+\frac{1}{r_2}\right) = \gamma\cdot\kappa, \tag{1}$$

where κ is a local boundary curvature.

A way to obtain an artificial driving force is to create a difference in free energy density across the boundary between two grains. For example, this can be accomplished by the application of a stress field to a polycrystal with an anisotropic Young's modulus or by exposing a polycrystal with an anisotropic dielectric susceptibility to an electrostatic field. The coupling of an appropriately directed external field with an anisotropic material's property will generate a free energy difference between adjacent grains that creates a driving force for boundary displacement. This driving force does not depend on boundary properties and moves a boundary from a grain with lower free energy towards one with a higher free energy.

In particular, such a condition can be obtained by the action of an external magnetic field on a crystalline material with an anisotropic magnetic susceptibility. As it has been initially shown by Mullins [4], the magnetic driving force $p_{\mathrm{m}}^{\mathrm{b}}$ on the boundary between two adjacent uniaxial crystals with different susceptibilities along the field direction and hence different magnetic energy densities, is given by

$$p_{\mathrm{m}}^{\mathrm{b}} = \frac{1}{2}\mu_0\Delta^2\left(\cos^2\theta_1-\cos^2\theta_2\right) \tag{2}$$

where μ_0 is the magnetic constant, $\Delta\chi = \left|\chi_{\parallel}\right| - |\chi_{\perp}|$ is the difference in susceptibility parallel $\chi_{\parallel}$ and perpendicular $\chi_{\perp}$ to the principal (or c) axis of the crystal, H is the magnetic field strength, θ_1 and θ_2 are the angles between the direction of the magnetic field and the principal axes of both neighboring grains.

The magnetic driving force reaches its maximum $p_{\mathrm{m}}^{\max} = \mu_0\Delta\chi H^2/2$, when the angles between the field and the c axes in both adjacent grains are $\theta_1 = 0$ and $\theta_2 = 90°$ or vice versa. The sign of $p_{\mathrm{m}}^{\mathrm{b}}$ depends on the magnetic anisotropy of the material ($\Delta\chi$) and the asymmetry of the spatial orientation of both neighboring grains with respect to the magnetic field direction. For a zero magnetic driving force the grain orientations do not need to be identical but merely to satisfy $\theta_1 = \theta_2$.

Being exposed to a magnetic field each grain of a polycrystal experiences a total magnetic driving force that can be expressed as the difference between the magnetic free energy density of this grain ω and an average magnetic free energy density $\bar{\omega}$ of its neighboring grains $p_{\mathrm{m}} = \omega - \bar{\omega}$. According to Eq. 2 this can be also written as

$$p_{\mathrm{m}} = \frac{1}{2}\mu_0\Delta\chi H^2\left(\cos^2\theta - \frac{\sum_n \cos^2\theta_n}{n}\right), \tag{3}$$

where θ and θ_n are the angles between the field direction and principal axes of the considered grain and its n neighboring grains.

The dependence of the magnetic driving force on the grain orientation explains why a magnetic field influences the orientation distribution in a polycrystal, or more specifically why it affects an existing texture or produces a preferred orientation in a structure with initially randomly oriented grains. Assuming $\Delta\chi > 0$, for a grain surrounded by its neighboring grains such that $\cos^2\theta - 1/n\cdot\sum_n \cos^2\theta_n < 0$, the magnetic energy density will be lower than the average energy density of the adjacent grains ($\omega < \bar{\omega}$) and in consequence the

magnetic driving force ($p_m < 0$) tends to expand this grain. For an aggregate of randomly oriented grains, whose angles between the c-axes and the field are described by a distribution $P(\theta) = 1/2 \sin\theta$ [16], the magnetic force can be expressed as

$$p_m^{\text{random}} = \frac{1}{2}\mu_0\Delta^2\left(\cos^2\theta - \frac{1}{2}\int_0^{\pi}\sin\theta\cdot\cos^2\theta\,d\theta\right) = \frac{1}{2}\mu_0\Delta\chi H^2\left(\cos^2\theta - \frac{1}{3}\right) \quad (4)$$

Therefore, assuming $\Delta\chi > 0$ as this is the case for Zn, Ti and Zr, grains with $\theta < \arccos 1\sqrt{3} \cong 55$ will initially be favored for growth, whereas grains with $\theta > 55°$ will be inclined to shrink by a magnetic driving force.

Kinetic equations

According to an approach proposed by Hillert [17], the rate of grain size change (dR/dt) under a curvature driving force can be expressed as

$$\frac{dR}{dt} = \alpha m_b \gamma\left(\frac{1}{\bar{R}} - \frac{1}{R}\right), \quad (5)$$

where the grain size is expressed by the radius R of a circle or sphere of the same area or volume, respectively, γ and m_b are the grain boundary energy and mobility (assumed equal for all grain boundaries) and α is a dimensionless constant. The mean grain size $\bar{R}$ denotes a critical size, such that at any time grains with $R > \bar{R}$ grow ($dR/dt > 0$), grains with $R < \bar{R}$ shrink ($dR/dt < 0$) and grains with $R = \bar{R}$ keep their size ($(dR/dt)_{R=\bar{R}} = 0$).

For the rate of grain size change under a magnetic driving force only one can write

$$\frac{dR}{dt} = -m_b p_m \quad (6)$$

According to Eq. 6 grains with a higher magnetic energy density ($p_m = \omega - \bar{\omega} > 0$) shrink, whereas grains with $\omega < \bar{\omega}$ expand.

The forces acting on a grain boundary during grain growth can safely be assumed additive [18, 19]. A summation of Eqs. 5 and 6 leads therefore to a kinetic equation for the case of a simultaneous action of both curvature and magnetic driving forces

$$\frac{dR}{dt} = \alpha m_b \gamma\left(\frac{1}{\bar{R}} - \frac{1}{R}\right) - m_b p_m \quad (7)$$

Obviously, a magnetic driving force superimposed to a curvature one during grain growth changes the size R_{th} of grains which neither grow nor shrink. This threshold size can be derived from

$$\left.\frac{dR}{dt}\right|_{R=R_{th}} = \alpha m_b \gamma\left(\frac{1}{\bar{R}} - \frac{1}{R_{th}}\right) - m_b p_m = 0, \quad (8)$$

and reads

$$R_{th} = \frac{\bar{R}}{1 - \frac{\bar{R}p_m}{\alpha\gamma}} \quad (9)$$

According to Eq. 9, the threshold grain size for grains with a lower magnetic free energy density ($p_m = \omega - \bar{\omega} < 0$) is reduced to $R'_{th} < \bar{R}$ (Fig. 1). Hence in contrast to a purely curvature driven grain growth, grains with a size $R'_{th} < R < \bar{R}$, which otherwise would shrink, will now expand due to the presence of a magnetic field. Opposite to this the threshold grain size for grains with a higher magnetic free energy density ($\omega > \bar{\omega}$) is increased to $R''_{th} > \bar{R}$ and therefore, grains with $\bar{R} < R < R''_{th}$, which otherwise would expand, will now shrink. From this it can be predicted that during magnetic annealing a smaller grain with $p_m < 0$ could grow at the expense of a bigger one for which $p_m > 0$.

The above analysis reveals that the texturing influence of a magnetic field is not only due to an increase in grain growth or shrinking rate, but also due to a change in fractions of differently oriented grains in a polycrystal. As a consequence of a shift in the threshold grain size in the field the number of growing grains with such orientation relationships to the field and their neighbors that they experience $p_m < 0$, will be larger than without field. On the other hand, more grains will shrink and disappear in the field than without it, for which due to their orientation relation-

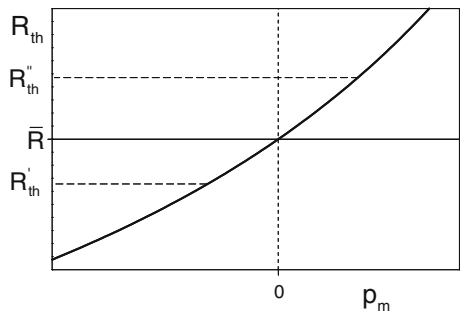

Fig. 1 Schematic dependence of a threshold grain size R_{th} on a magnetic driving force p_m, as given by Eq. 9

ships a force $p_m > 0$ is induced. Obviously this must result in an increase or decrease of differently oriented grain fractions.

An alternative topological approach for grain growth in 2D systems was developed by Mullins [20], who applied von Neumann's description of a 2D soap froth [21] to curvature driven grain growth. Also here all boundaries were assumed to possess equal energy γ and mobility m_b, and considered to be in equilibrium at their triple junctions. A possible dragging impact of triple junctions on the boundary motion was disregarded. According to this approach there is a unique relation between the rate of area change dS/dt and the topological class n (number of next neighbors) of a grain. Grains with $n > 6$ will grow, and those with $n < 6$ will disappear [20].

$$\frac{dS}{dt} = \frac{\gamma m_b \cdot \pi}{3}(n-6) \tag{10}$$

It can be easily shown that this relation will be violated in the presence of a magnetic field. Consider a 2D grain of area S bordered by curved grain boundaries. If this grain shrinks, a boundary element $\Delta\ell$ moving with a normal velocity v will sweep in a time interval Δt an area element $\Delta S = v \cdot \Delta t \cdot \Delta\ell$. Thus the rate of the area change for the whole grain can be defined by

$$\frac{dS}{dt} = -\oint v\, d\ell \tag{11}$$

In the presence of a magnetic field v is determined by both curvature and an additional magnetic driving force $v = \gamma m_b \cdot \kappa + m_b p_m)$. With the boundary curvature κ, defined as a change of the tangential angle ϕ along the boundary $\kappa = d\varphi/d\ell$, the rate of the grain area change then reads

$$\begin{aligned}\frac{dS}{dt} &= -\oint (\gamma m_b \cdot \kappa + m_b p_m) d\ell \\ &= -\gamma m_b \oint d\varphi - m_b p_m \oint d\ell\end{aligned} \tag{12}$$

For a completely continuous grain boundary the first integral $\oint d\varphi$ in the right part of Eq. 12 would equal 2π. However due to a discontinuous change of the angle at every triple junction a half of the equilibrium angle $2\pi/3$ has to be substracted from the total value of 2π for each junction [20]. The second integral $\oint d\ell$ over the grain is equal to the grain perimeter Π. Consequently Eq. 12 can be simplified as

$$\frac{dS}{dt} = m_b\left[\frac{\pi\gamma}{3}(n-6) - p_m\Pi\right] \tag{13}$$

Switching to an equivalent grain size (radius R of a circular grain of the same area) and substituting $S = \pi R^2$ and $\Pi = 2\pi R$ we arrive at

$$\frac{dR}{dt} = m_b\left[\frac{\gamma}{R}\left(\frac{n}{6}-1\right) - p_m\right] \tag{14}$$

The topological class n_{th} of stable grains of size R_{th} can now be derived from the condition

$$m_b\left[\frac{\gamma}{R_{th}}\left(\frac{n_{th}}{6}-1\right) - p_m\right] = 0, \tag{15}$$

and reads

$$n_{th} = 6\left(1 + \frac{R_{th}P_m}{\gamma}\right) \tag{16}$$

According to Eq. 14, the topological class of stable grains with a lower magnetic free energy density than their immediate surroundings, ($p_m < 0$), is reduced to $n_{th} < 6$ and vice versa raised to $n_{th} > 6$ for grains with a higher energy ($p_m > 0$) (Fig. 2).

Substituting the expression for R_{th} (Eq. 9) into Eq. 16 and taking into account that for a 2D grain system $\alpha \cong 0.5$ [17], one finds for the threshold topological class

$$n_{th} = 6\left(\frac{\gamma - \bar{R}p_m}{\gamma - 2\bar{R}p_m}\right) \tag{17}$$

A possible absolute deviation of n_{th} from $n = 6$ can be estimated for the practical case of grain growth in α-titanium ($\Delta\chi_{Ti} = 1.18 \cdot 10^{-5}$[22]) in a field of 19.4 T [13]. According to Eqs. 2 and 3 the magnetic driving

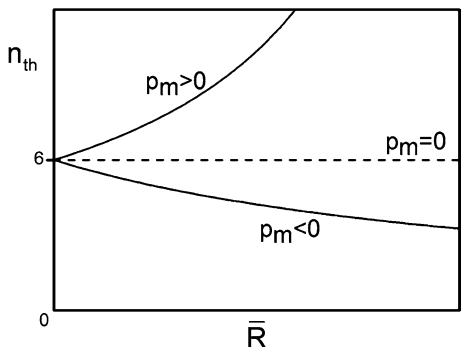

Fig. 2 Topological class of stable grains versus mean grain size, as given by Eq. 17

force for such estimation can be taken as $p_m \cong 10^3$ J/m^3. For a typical grain boundary energy γ in Eq. 17 of 0.4 J/m^2 and a mean grain size of about 80 μm (see Sect. 3 of the current paper), i.e. $\bar{R} \cong 40$ μm, the threshold topological class for stable grains with $p_m = -1.0$ kJ/m^3 amounts 5.5 and for grains with $p_m = +1.0$ kJ/m^3 – 6.75.

Magnetically affected grain growth: experiment

As has been shown in the previous section, a magnetic driving force superimposed to a curvature driving force during grain growth can bias the microstructure evolution with respect to size and orientation distribution of grains. Experimentally it has been demonstrated first on grain growth in zinc [12]. Annealing of cold-rolled zinc sheet without a field results in a regular texture with two symmetrical components in the {0002} pole figure (Fig. 3a). If, however, the annealing occurs in a magnetic field and the sample is specifically oriented with respect to the field direction, one or another texture component can be amplified that eventually results in a single-component texture (Fig. 3b, c).

Similar results, i.e. strengthening of one and weakening of another component in a sharp two-component texture, were observed in further experiments on cold-rolled α-titanium [13, 14] and, quite recently, cold-rolled zirconium [15]. The specimens during magnetic annealing were oriented in such a manner that the *c*-axes of grains which make up one texture component (in zinc around the orientations $\{\phi_1 = 90°, \Phi = 20°, \forall\phi_2\}$ (Fig. 3b) or $\{\phi_1 = 270°, \Phi = 20°, \forall\phi_2\}$ (Fig. 3c) [12], in titanium – $\{\phi_1 = 180°, \Phi = 30°, \forall\phi_2\}$ (Fig. 4) [14] or $\{\phi_1 = 0°, \Phi = 30°, \forall\phi_2\}$ [11]) were directed perpendicular to the field direction. With $\Delta\chi > 0$ for zinc, titanium and zirconium, the magnetic free energy density of many grains in this component approaches a minimum that results in an additional driving force for their growth ($p_m < 0$).

The intensity of a texture peak measured by X-ray diffraction can be estimated as the product of the mean area and the number (or fraction) of grains which make up that peak. In order to separate the contribution of these parameters to the texture changes, individual orientations were measured by electron back scattering diffraction in a scanning electron microscope [11, 14]. The results revealed that the mean size of grains for which $p_m < 0$ (more intense component {0°, 30°, $\forall\phi_2$} in [14] (Fig. 4)) only slightly exceeds the mean size of grains of the another component. In contrast, fully in accordance with predictions of the previous section, fractions of grains in both texture components were found to be drastically different (0.32–0.65 after 15 min annealing at 750 °C in a field of 19.4 T [14]). As was shown above, the threshold grain size R_{th} is increased in the high energy component ($p_m > 0$), whereas it is decreased in the low energy component. As a result, more grains of the high energy component shrink and disappear as it would be the case without a magnetic field. Vice versa, more grains of the low energy component ($p_m < 0$) will grow in the presence of a magnetic field. From this it can be concluded that the texture asymmetry caused by a magnetic field stems to a great extent from this difference in grain fractions.

Magnetically affected grain growth: 2D computer simulations

In order to prove the validity of theoretical predictions and to analyze experimental results by an independent method we employed computer simulations of 2D grain growth. The simulation algorithm is based on vertex and front-tracking models which are most appropriate for curvature and boundary tension driven grain growth [23–26]. The grain structure in this algorithm is represented by differently oriented grains, separated by boundaries that intersect at triple

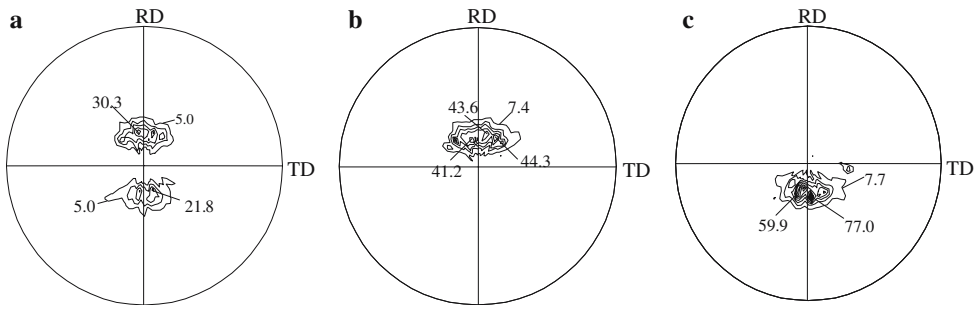

Fig. 3 {0002} pole figures of 99%-rolled zinc–1.1% aluminum sheet samples (**a**) after annealing at 390 °C without a magnetic field, in a magnetic field of 32 T with rolling direction (RD) tilted by +19° to the field around transverse direction (TD) (**b**) and tilted by – 19° to the field around TD (c) [12]

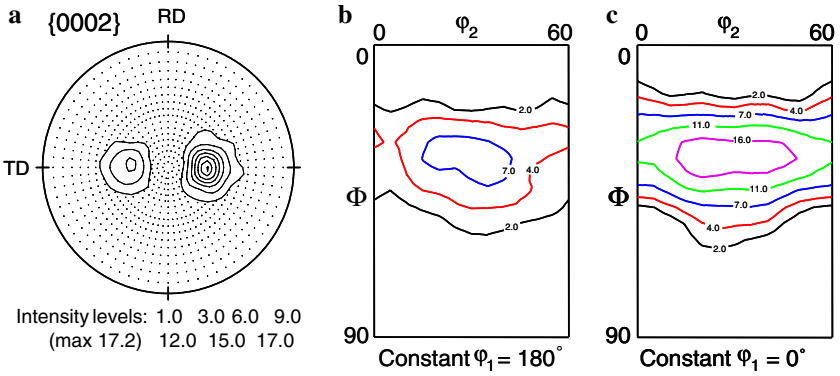

Fig. 4 {0002} pole figure (**a**), $\varphi_1 = 180$ (**b**) and $\varphi_1 = 0$ (**c**) ODF (orientation distribution function) sections for 75% cold-rolled Ti sheet after 15 min magnetic annealing at 750 °C in a magnetic field of 19.4 T [14]

junctions (real vertices). The grain boundaries in turn consist of points (virtual vertices) along the boundary length according to the boundary curvature [27]. During grain growth without an external field all boundary points move under a curvature driving force p_c in a normal direction according to the local boundary curvature (Eq. 1). In the presence of a magnetic field the equation $v = m_b p$ of boundary motion is solved for all boundary points with a driving force equal to the sum of curvature and magnetic driving forces $p = p_c + p_m$, where p_m is calculated according to Eq. 2 [27].

In Figs. 5 and 6 the simulated grain structure evolution of a 2D polycrystal is presented. The microstructure of this polycrystal was developed under a pure curvature driving force. Figure 5 shows the computed time dependence of the normalized mean grain area. As seen, the mean grain area increases linearly with annealing time. According to theory this behavior is characteristic for normal grain growth driven by a change of the grain boundary energy due to a reduction of the grain boundary area. Furthermore it was assessed whether the model reproduces a topological microstructure evolution according to the von Neumann–Mullins relation (Eq. 10). The computed dependence of the rate of grain area change dS/dt on the topological class n of a grain is shown in Fig. 6. The agreement between the classical relation (Eq. 10) dS/dt $\approx 1.047\ m_b\gamma(n - 6)$ [20] and the linear fit of the simulated results dS/dt = $1.044\ m_b\gamma(n - 6.0029)$ is remarkable. Therefore, the results shown in both Figs. 5 and 6 convincingly demonstrate the validity of the used simulation model to study grain growth in 2D homogeneous systems.

For simulations of magnetically affected grain growth the experimental conditions were reproduced. The initial microstructure was reconstructed from individual orientation data (EBSD mapping) measured on a recrystallized Ti sample with a mean grain size of 42 μm. Grain boundary energy and mobility in the current simulations were assumed to be uniform. A magnetic field was applied perpendicular to the rolling direction of the specimen and tilted to its transverse direction by 30°, as indicated by a cross in the pole figure in Fig. 7b. Therefore, according to our understanding, depending on their surroundings, many

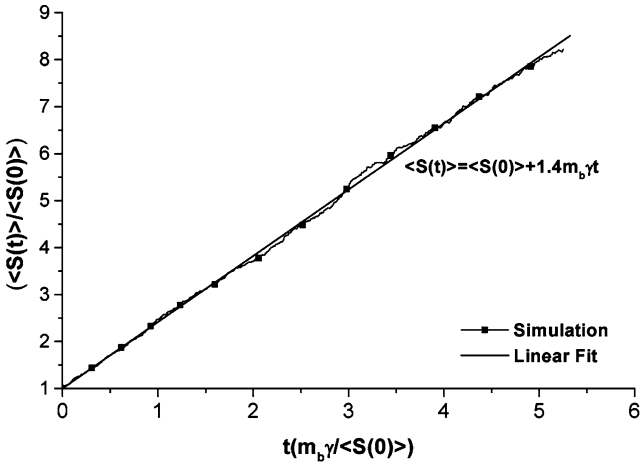

Fig. 5 Computed normalized grain area $S(t)/S(0)$ versus time

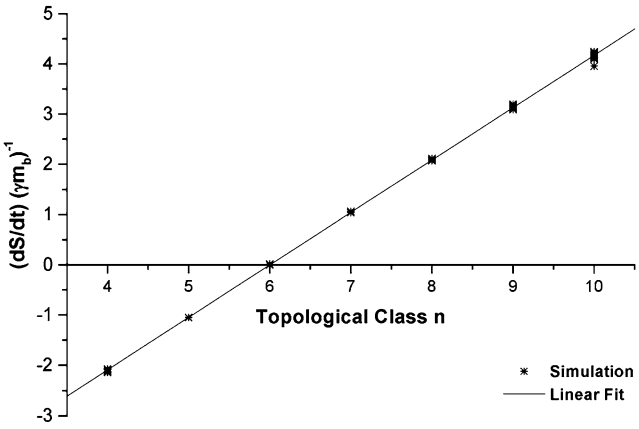

Fig. 6 The rate of grain area change dS/dt as function of the topological class n of a grain

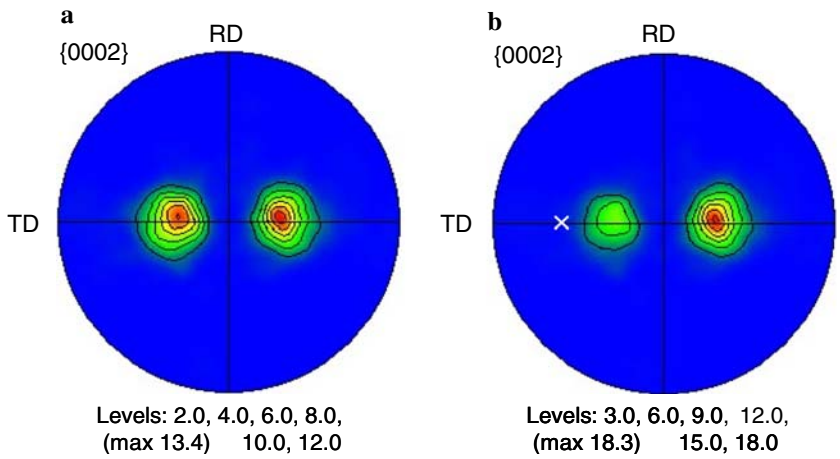

Fig. 7 Simulated {0002} pole figures after 600 s annealing at 750 °C for a 2D Ti-polycrystal (**a**) without field and (**b**) in a magnetic field of 19.4 T (field direction is indicated by a white cross)

grains of the {0°, 30°, $\forall\phi_2$} component are expected to experience an additional on growth directed magnetic driving force ($p_m < 0$), since their *c*-axes are aligned nearly normal to the field direction.

Figures 7–9 show the simulation results. Excellent agreement between simulations and experiment was obtained in almost all respects. Specifically, after annealing at zero field the simulated texture remains symmetrical, while after magnetic annealing one texture component (in the current case {0°, 30°, $\forall\phi_2$} with *c*-axes perpendicular to the field) becomes much stronger than the other component. Further, as shown in Fig. 8, the grain fraction of the energetically advantaged component ($p_m < 0$) rises during the annealing in the field, whereas the grain fraction of the other component decreases.

The simulations also fully confirm the theoretical predictions concerning the magnetically affected grain topology. According to the analysis given in the 'Driving forces' section (Eqs. 12–17), the von Neumann–Mullins relation is violated in the presence of an external magnetic field: grains with the topological class $n = 6$ do not remain stable anymore. Depending on their orientation and orientation of their direct neighbors with respect to the field direction, all grains including those with topological class $n = 6$ become either favored or disfavored by a magnetic field. As a consequence, grains with $n = 6$ in favorable orientations grow, whereas grains with $n = 6$ in unfavorable configurations shrink (Fig. 9).

Figure 10 demonstrates that, although growth kinetics is distinctly different for differently oriented grains, the total grain growth kinetics is not significantly affected by a magnetic field. However, the simulations shown in Figs. 8 and 9 substantiate that a magnetic field not only slows down or increases the growth rate of differently oriented grains, but also changes the grain microstructure of 2D polycrystals.

Summary

In addition to a curvature driving force during grain growth, a magnetic driving force arises in a polycrystalline solid with anisotropic magnetic susceptibility when exposed to a magnetic field. This force stems from a difference in magnetic free energy density across the boundary and acts supplementary to a curvature driving force. With or against the curvature driving force it additionally impels each grain of a

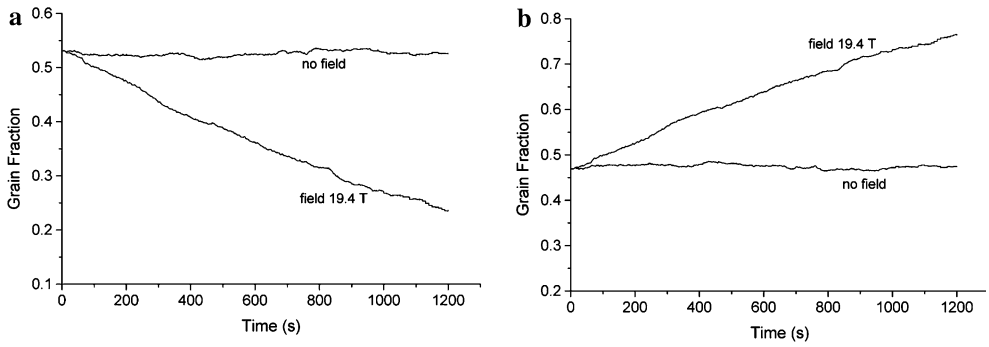

Fig. 8 Computed grain fractions in (**a**) {180°, 30°, $\forall\phi_2$} grain subset and (**b**) {0°, 30°, $\forall\phi_2$} grain subset versus annealing time at zero field and in a field of 19.4 T

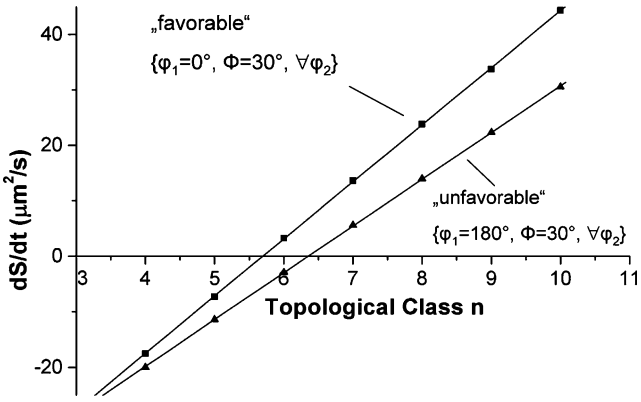

Fig. 9 Computed rate of grain area change for differently oriented grains after 300 s annealing at 750 °C in a field of 19.4 T

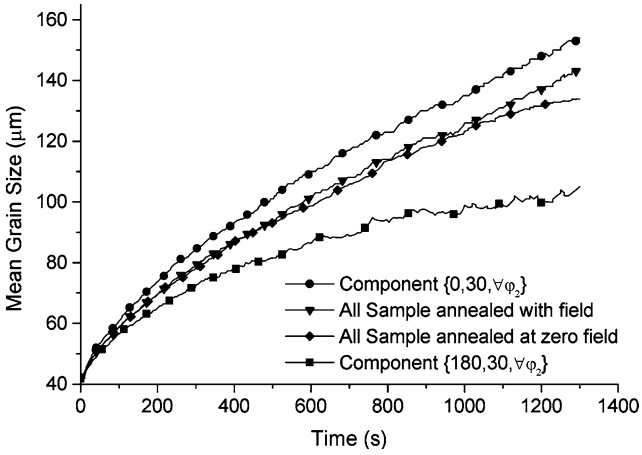

Fig. 10 Simulated grain growth kinetics for the magnetically annealed specimen

polycrystal to grow or to shrink, depending on its orientation and the orientation of its nearest neighbors with respect to the field direction. Owing to the orientation dependency of the magnetic driving force, a magnetic field possesses a remarkable property to produce preferred orientations during grain growth.

A theoretical analysis of the grain growth kinetics reveals that the classical conditions for a grain to retain its size stable—to have a size equal to the mean grain size, as follows from the Hillert equation, or to possess a topological class equal 6, as it follows from the von Neumann–Mullins approach, are violated in the presence of an external magnetic field. The extended Hillert equation reveals that for grains in favorable energetic configurations the treshold grain size rises compared to the mean grain size, but it decreases for grains with higher magnetic energy. Analogously in an extended von Neumann–Mullins approach, depending on their orientation all grains including those with topological class 6 become either advantaged or disadvantaged by a magnetic field. As a consequence grains with topological class 6 do not remain stable in the field, but either grow or shrink.

As it is experimentally demonstrated on polycrystalline zinc, titanium and zirconium sheet, the crystallographic texture in magnetically anisotropic dia- or paramagnetic materials can be effectively changed and controlled by means of magnetic annealing. EBSD-analysis revealed that the observed asymmetrical texture after magnetic annealing is due to a large extent to a significant difference in the number of grains making up different texture components.

The results of computer simulations of magnetically affected grain growth in 2-D polycrystals are in a good agreement with theoretical predictions and experimental findings; a development of an asymmetrical texture with a rising difference between grain fractions in different texture components as well as a change of the topological class of stable grains depending on their orientations is convincingly demonstrated.

Acknowledgements The authors express their gratitude to the Deutsche Forschungsgemeinschaft for financial support (Grant MO 848/6-1). Part of this work was performed at the National High Magnetic Field Laboratory, which is supported by NSF (Cooperative Agreement No. DMR-0084173), by the State of Florida and by the DOE. Helpful and stimulated discussions with Profs. G. Gottstein, L. S. Shvindlerman, V. Yu. Novikov, C. Krill and P. Streitenberger are gratefully acknowledged. L.A.B.-M. conveys his thanks to the Deutscher Akademischer Austauschdienst (DAAD) for his Ph.D. stipend.

References

1. McLean M (1982) Metal Sci 16:31
2. T Watanabe (2001) In: Gottstein G, Molodov DA (eds) Recrystallization and grain growth. Springer, Berlin, p 11
3. Deus AM, Fortes MA, Ferreira PJ, Vander Sande JB (2002) Acta Mater 50:3317
4. Mullins WW (1956) Acta Metall 4:421
5. Fraser MJ, Gold RE, Mullins WW (1961) Acta Metall 9:960
6. Molodov DA, Gottstein G, Heringhaus F, Shvindlerman LS (1997) Scripta Mater 37:1207
7. Molodov DA, Gottstein G, Heringhaus F, Shvindlerman LS (1998) Acta Mater 46:5627
8. Sheikh-Ali AD, Molodov DA, Garmestani H (2003) Appl Phys Lett 82:3005–3007
9. Konijnenberg PJ, Molodov DA, Gottstein G (2005) In: NHMFL 2004 Annual Research Review. NHMFL, Tallahassee, p 15. http://www.magnet.fsu.edu/publications/2004annualreport/reports/2004-NHMFL-Report137.pdf
10. Konijnenberg PJ, Molodov DA, Gottstein G (2004) Mater Sci Forum 467–470:763
11. Molodov DA, Konijnenberg PJ (2005) Z Metallkd 96:1158
12. Sheikh-Ali AD, Molodov DA, Garmestani H (2002) Scripta Mater 46:857
13. Molodov DA, Sheikh-Ali AD (2004) Acta Mater 52:4377

14. Molodov DA, Konijnenberg PJ, Bozzolo N, Sheikh-Ali AD (2005) Mater Lett 59:3209
15. Molodov DA, Konijnenberg PJ, Bozzolo N, will be published
16. Weisstein EW In: Mathworld – a Wolfram web resource. http://mathworld.wolfram.com/SpherePointPicking.html
17. Hillert M (1965) Acta Metall 13:227
18. Novikov VYU (1999) Acta Mater 47:4705
19. Gangulee A (1974) J Appl Phys 45:3749
20. Mullins WW (1956) J Appl Phys 27:900
21. Von Neumann J (1952) In: Metal interfaces. American Society for Testing Materials, Cleveland, p 108
22. Volkenshtein NV, Galoshina EV, Panikovskaya EB (1975) Sov Phys JETP 40:730
23. Kawasaki K, Nagai T, Nakashima K (1989) Phil Mag 60:339
24. Weigand D, Brechet Y, Lepinoux J (1998) Phil Mag B 78:329
25. Frost HJ, Thompson CV, Howe CL, Wang J (1998) Scripta Metall Mater 22:65
26. Fayad W, Thompson CV, Frost HJ (1999) Scripta Mater 40:1199
27. Barrales-Mora LA, Mohles V, Konijnenberg PJ, Molodov DA (2006) Comp Mater Sci In press